

Discrete Spatio-Temporal State Estimation via Reduced Order Models of the Heat Equation

Fernando López-Caamal* Ixbalank Torres**
Sergio Cano-Andrade***

* *Department of Chemical Engineering, Universidad de Guanajuato,
Guanajuato, GTO 36050, Mexico*

** *Department of Electronics Engineering, Universidad de Guanajuato,
Salamanca, GTO 36885, Mexico*

*** *Department of Mechanical Engineering, Universidad de
Guanajuato, Salamanca, GTO 36885, Mexico*

Abstract:

In this paper, we address the problem of estimating the value of a spatio-temporal signal at locations where no information is available. The evolution of the signal is described by a one-dimensional heat equation with a nonlinear source term. We use the Laplacian spectral decomposition methodology to design an observer capable of estimating the value at both discrete locations of the space and in discrete time. To show applicability of the methodology, we consider the heat transfer in an injection mold represented by a homogeneous bar subject to joule heating effect.

Keywords: Heat equation, Laplacian operator, LSD, Discrete Luenberger observer.

1. INTRODUCTION

Injection molding has become a successful manufacturing process for mass production due to the ability to scale production of complex parts in large volume at a low production cost. However, nowadays, injection molding still has several limitations due to temperature, pressure, injection speed, among others (Hwang, 2012; Goodship, 2004). The effect that the largest impact has on this process is the mold temperature. Several characteristics of the manufactured pieces depend on this variable, such as the tensile modulus and the flexural modulus (Zheng et al., 2017), the organization of the core layers during crystallization (Jiang et al., 2015), particle orientation and packing (Bianchi et al., 2019), and chemical foaming of injection molded recycled polyethylene-terephthalate and its porosity relation (Ronkay et al., 2017). Besides, the polymer crystallinity increases at higher mold temperatures and, if the temperature is not controlled, crystal growth can generate a defective piece (Renterghem et al., 2018). Controlling and monitoring online the mold temperature, which vary along both space and time, during injection is therefore a very important issue.

To this end, (Mamoun and Tapan, 2015) propose a control mold surface system where the temperature is controlled by means of an automatic control algorithm and measured by thermocouples. (Fan and Gao, 2006) present the design and performance analysis of a sensor in which temperature and pressure are measured inside the mold cavity,

optimizing the mold temperature performance. (Demirel, 2017) propose the optimization of the mold surface in order to control the injection and crystallization process to improve the surface finish.

Progression of spatio-temporal signals in a homogeneous media may be properly modeled via partial differential equations (PDEs). The Laplacian spectral decomposition (LSD) methodology is a Galerkin method that uses of the properties of the Laplacian to represent the PDE as a set of ODE's of larger dimensions whose solution assists on the approximation solutions of PDE driven by the Laplacian operator (Courant and Hilbert, 1937; García, 2008; Christofides, 2012; Grebenkov and Nguyen, 2013).

On the other hand, when measurements of signals are not available online (for controlling or monitoring purposes), observers can be considered to online estimate them (the temperature along the mold surface, for instance). The main task of an observer is to estimate unmeasured information provided a (partially) known dynamical system, along with its inputs and some measured outputs. Within the PDE context, an observer may be used to estimate the value of a state at locations where no information is available, given the availability of online measurements at specific locations. In the following we adopt such a perspective. Other observation problems in distributed parameters systems are presented by (Llu and Lapdus, 1976; Zuazua, 2007; Wouwer and Zeitz, 2009; Hidayat et al., 2011).

In (Torres et al., 2010) the authors use the proper orthogonal decomposition method to estimate the value of states at unknown locations. In turn, the authors of (López-Caamal and Moreno, 2015) use the LSD method to estimate unmeasured states, given the continuous measurement of some states. The problem of determining the location of sensors, to maximize the information reconstructed by the measured information have been studied, for instance, in (García et al., 2007).

In this paper we design an observer capable of estimating the state at unmeasured locations of a unidimensional dynamic heat equation with a nonlinear source function. We use a linear observer to obtain such measurements in discrete time. To assess the performance of our observer, we use the finite element method to approximate the solution of the considered PDE, see for instance (Chandrupatla et al., 2002; Vilas Fernández, 2008). Our case study is the temperature distribution in an injection mold represented by a homogeneous steel bar subject to heating due to an electric current. We consider that the bar is isolated on its boundaries and the only available measurements are at the extreme points of the bar.

This paper is organized as follows: in Section 2 the concepts around which the proposed observer is designed are introduced. Section 3 depicts the design of the proposed observer. In Section 4 the PDE-based model of a steel bar (the study case) is introduced. In Section 5 a comparison between model and observer simulations are presented and discussed. Finally, Section 6 states some conclusions about the feasibility of the proposed estimation strategy.

1.1 Notation

In what follows $f[\circ]$ denotes a function of a discrete argument; whereas $h(\circ)$, a function of continuous one. In turn, the continuous time is denoted by t ; whereas the discrete time is denoted by k . Thus $h(t)$ is a function of continuous time and $f[k]$ is a discrete-time one.

2. BACKGROUND

In this section we introduce the concepts upon which we build our observer.

2.1 Laplacian Spectral Decomposition

Consider a Hilbert space over the spatial domain Ω endowed with the inner product

$$\langle f(x), g(x) \rangle := \int_{\Omega} g^{\top}(x) f(x) dx,$$

where $x \in \Omega$. Also consider the set of functions $\{\phi_i(x)\}_{j=1}^{\infty}$, where $\phi_i(x) : \Omega \rightarrow \mathbb{R}$. Let this set be complete and thus a basis for the Hilbert space.

Furthermore, the LSD approach considers such $\phi_i(x)$'s that

(1) are eigenfunctions of the Laplacian operator

$$\nabla^2 \phi_i(x) = \lambda_i \phi_i(x) \quad (1a)$$

subject to particular boundary conditions;

(2) and the eigenfunctions are orthonormal to each other:

$$\langle \phi_i(x), \phi_j(x) \rangle = \delta_{i,j}, \quad (1b)$$

where $\delta_{i,j}$ is the Kronecker delta.

Now, the LSD method avails of such functions in order to express a spatio-temporal signal as follows

$$z(t, x) = \sum_{i=1}^{\infty} w_i(t) \phi_i(x), \quad (2)$$

where $w_i(t)$ are called the weights and are given by

$$w_i(t) := \langle z(t, x), \phi_i(x) \rangle. \quad (3)$$

By truncation of the infinite sum in (2), one may approximate $z(t, x)$ as

$$z(t, x) \approx \mathbf{w}_z^{\top}(t) \phi(x), \quad (4)$$

where $\phi(x) : \Omega \rightarrow \mathbb{R}^{\vartheta}$ is a vector composed of the first ϑ elements of $\{\phi_i(x)\}_{j=1}^{\infty}$. Likewise, the i^{th} entry of $\mathbf{w}_z^{\top}(t)$ is the weight of $z(t, x)$ w.r.t. the i^{th} basis element.

A hallmark of the approximation in (4) is its behavior w.r.t. the Laplacian operator:

$$\begin{aligned} \nabla^2 z(t, x) &\approx \nabla^2 \left(\mathbf{w}_z^{\top}(t) \phi(x) \right) \\ &= \mathbf{w}_z^{\top}(t) \nabla^2 \phi(x) \\ &= \mathbf{w}_z^{\top}(t) \mathbf{\Lambda} \phi(x), \end{aligned} \quad (5)$$

where $\mathbf{\Lambda} \in \mathbb{R}^{\vartheta \times \vartheta}$ is a diagonal matrix composed of the eigenvalues λ_i in (1a).

2.2 Observers of Discrete Time LTI Systems

Let us consider a discrete-time linear system of the form

$$\mathbf{x}[k+1] = \mathbf{E}\mathbf{x}[k] + \mathbf{B}\mathbf{u}[k] \quad (6a)$$

$$\mathbf{y}[k] = \mathbf{F}\mathbf{x}[k], \quad (6b)$$

where $\mathbf{x}[k] : \mathbb{N} \rightarrow \mathbb{R}^n$ and $\mathbf{y}[k] : \mathbb{N} \rightarrow \mathbb{R}^m$ denotes the measured states. The rest of the matrices are of appropriate dimensions. Furthermore, let us consider the observability matrix:

$$\mathcal{O} := \begin{pmatrix} \mathbf{F} \\ \mathbf{FE} \\ \vdots \\ \mathbf{FE}^{n-1} \end{pmatrix}, \quad (7)$$

where n is the order of the matrix \mathbf{E} . A necessary and sufficient condition to determine the vector $\mathbf{x}[k]$ via the online knowledge of $\mathbf{y}[k]$ is

$$\text{rank}(\mathcal{O}) = n.$$

Now, an observer is a dynamical system capable of estimating $\mathbf{x}[k]$ given the online measurement of the input and output to the observed system. A common approach is to consider a copy of the system plus a properly designed output error injection. That is to say, an observer to (6) may have the form

$$\begin{aligned} \hat{\mathbf{x}}[k+1] &= \mathbf{E}\hat{\mathbf{x}}[k] + \mathbf{B}\mathbf{u}[k] - \mathbf{L}(\hat{\mathbf{y}}[k] - \mathbf{y}[k]) \\ \hat{\mathbf{y}}[k] &= \mathbf{F}\hat{\mathbf{x}}[k]. \end{aligned}$$

3. REDUCED ORDER DISCRETE OBSERVER

Let us consider the following PDE

$$\frac{\partial}{\partial t} z(t, x) = \alpha \nabla^2 z(t, x) + f(t, x). \quad (8a)$$

subject to boundary and initial conditions. The spatial domain that we consider is $\Omega = [0, 1]$, and $z, f : \mathbb{R}_+ \times \Omega \rightarrow \mathbb{R}$ and $\alpha \in \mathbb{R}_+$. In addition, let \mathbf{x} be a vector which represents discrete locations within the spatial domain; likewise $\mathbf{x}_m = (x_i)_{i=1}^\ell$ is a column vector composed of the locations where $z(t, x)$ is known. The entries of \mathbf{x} may be regarded as the locations at which one requires to know the signal $z(t, x)$.

Now, let $\mathbf{z}[t, \mathbf{x}]$ be a vector composed with the value of $z(t, x)$ at the locations that compose \mathbf{x} . Thus, the system's output is given by

$$\mathbf{y}[t, \mathbf{x}_m] = \mathbf{C}\mathbf{z}[t, \mathbf{x}]. \quad (8b)$$

Here, the matrix \mathbf{C} selects the locations at which $\mathbf{z}[t, \mathbf{x}]$ is known.

The following observer provides an estimation of $\mathbf{z}[t, \mathbf{x}]$ given $\mathbf{y}[t, \mathbf{x}_m]$. We denote such an estimation with $\hat{\mathbf{z}}[t, \mathbf{x}]$.

Proposition 1. Consider System (8). Let

$$\Phi^\top[\mathbf{x}_m] := (\phi[x_1] \dots \phi[x_\ell])^\top \quad (9)$$

$$\mathbf{A} := \alpha \mathbf{\Lambda} \quad (10)$$

$$\mathbf{C}_e := \mathbf{C}\Phi^\top[\mathbf{x}_m], \quad (11)$$

where the pair $(\mathbf{A}, \mathbf{C}_e)$ is observable. Then $\hat{\mathbf{z}}[t, \mathbf{x}] = \Phi^\top[\mathbf{x}]\hat{\mathbf{w}}_z(t)$, where $\hat{\mathbf{w}}_z(t)$ are the solutions of

$$\frac{d}{dt} \hat{\mathbf{w}}_z(t) = \mathbf{A}\hat{\mathbf{w}}_z(t) + \mathbf{w}_f(t) - \mathbf{L}(\hat{\mathbf{y}}[t, \mathbf{x}_m] - \mathbf{y}[t, \mathbf{x}_m]) \quad (12a)$$

$$\hat{\mathbf{y}}[t, \mathbf{x}_m] = \mathbf{C}_e \hat{\mathbf{w}}_z(t) \quad (12b)$$

and \mathbf{L} is as in (5). Furthermore, \mathbf{L} is any matrix that renders the matrix $\mathbf{A} - \mathbf{L}\mathbf{C}_e$ stable.

Proof. See Appendix A.

When a time-continuous knowledge of $\mathbf{y}[t, \mathbf{x}_m]$ is unfeasible, one may also consider a discrete measurement in time. For the sake of simplicity, we further assume that the time-sampling period is constant and denoted by τ ; thus $t = k\tau$, where k is a discrete variable. By applying Euler's discretisation method, Equation (12) becomes

$$\hat{\mathbf{w}}_z[k+1] = \mathbf{A}_d \hat{\mathbf{w}}_z[k] + \tau \mathbf{w}_f[k] - \mathbf{L}_d (\hat{\mathbf{y}}[k, \mathbf{x}_m] - \mathbf{y}[k, \mathbf{x}_m]) \quad (13a)$$

$$\hat{\mathbf{y}}[k, \mathbf{x}_m] = \mathbf{C}_e \hat{\mathbf{w}}_z[k] \quad (13b)$$

$$\hat{\mathbf{z}}[k+1, \mathbf{x}] = \Phi^\top[\mathbf{x}]\hat{\mathbf{w}}_z[k+1], \quad (13c)$$

where

$$\mathbf{A}_d := \tau \mathbf{A} + \mathbf{I} \quad (14a)$$

$$\mathbf{L}_d := \tau \mathbf{L} \quad (14b)$$

$$\mathbf{w}_{f,i}[k] := \langle f(k\tau, x), \phi_i(x) \rangle. \quad (14c)$$

Proposition 2. By appropriately designing the matrix \mathbf{L}_d System (13) is an observer for (8).

Proof. See Appendix B.

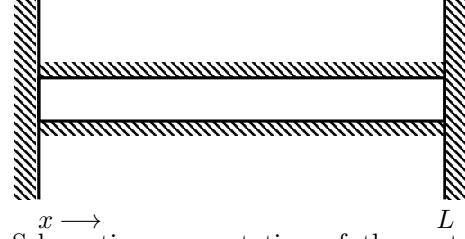


Fig. 1. Schematic representation of the system under study.

4. CASE OF STUDY

If we assume that the injection mold is homogeneous in both, composition and geometry, we may consider for the analysis only a small part of it. Such a section can be represented by a bar that is in contact with the injection material at one end, allowing the heat transfer from the material to the bar. The other surfaces can be considered to be isolated due to the symmetry condition.

Figure 1 shows the simplified version of the system under study. The system represents a square bar of steel, with $L = 1$ m, which is initially at a uniform temperature of $T_0 = 298$ K. The boundaries of the steel piece are thermally insulated. Then, an electric current is introduced to the bar at $x = L/2$, which produces an internal heat generation $q_{\text{gen}}(x)$. The block has a conductivity $k = 63.9$ W/m K, a density $\rho = 7832$ kg/m³, and a specific heat $c = 434$ J/kg K.

The law of conservation of thermal energy for differential control volumes is given as

$$\rho c \frac{\partial T}{\partial t} = -\nabla \cdot \mathbf{q} + q_{\text{gen}}(x) \quad (15)$$

and Fourier's law for a homogeneous isotropic solid with constant properties, is given as

$$\mathbf{q} = -k \nabla T. \quad (16)$$

By using Fourier's law in Equation (15), it becomes

$$\rho c \frac{\partial T}{\partial t} = k \nabla^2 T + q_{\text{gen}}(x). \quad (17)$$

Since we consider a unidimensional spatial domain Equation (17) is written as

$$\rho c \frac{\partial T}{\partial t} = k \frac{\partial^2 T}{\partial x^2} + q_{\text{gen}}(x) \quad (18)$$

or written in compact form, the governing equation is

$$\frac{\partial T}{\partial t} = \frac{k}{\rho c} \frac{\partial^2 T}{\partial x^2} + \frac{1}{\rho c} q_{\text{gen}}(x). \quad (19)$$

The internal generation of energy is approximated by

$$q_{\text{gen}}(x) = q_0 \left[1 - \left(\frac{x}{L} \right)^2 \right], \quad (20)$$

where $q_0 = 5000$ W/m³ is the local rate of energy generation. The initial condition is

$$T(x, 0) = T_0 \quad (21)$$

and the boundary conditions are

$$\left. \frac{dT}{dx} \right|_x = 0 \quad (22)$$

at $x = 0$ and $x = L$, which represent an insulated surface.

5. RESULTS AND DISCUSSION

In order to simulate the steel bar introduced in the previous section, the PDE (19) was numerically solved by the finite element method (FEM). The spatial domain was discretized in 51 points, while a sample period $\tau = 1s$ was considered. This way, the PDE (19) was approximated by the system of ODEs

$$\frac{d}{dt}T_x(t) = -MM^{-1} \left(\left(\frac{k}{\rho c} DM \right) + BM \right) T_x(t) + \frac{1}{\rho c} q_{\text{gen}}(x),$$

where T_x is a vector of temperatures along the space domain. Besides, MM , DM and BM are the mass, diffusion and boundary matrices, computed by using the *MATFEM* library (Vilas Fernández, 2008). The precedent ODE system was solved by the stiff solver *ode15s* for a time interval of 1 hour. The results of such an approach are displayed in Figure 2.

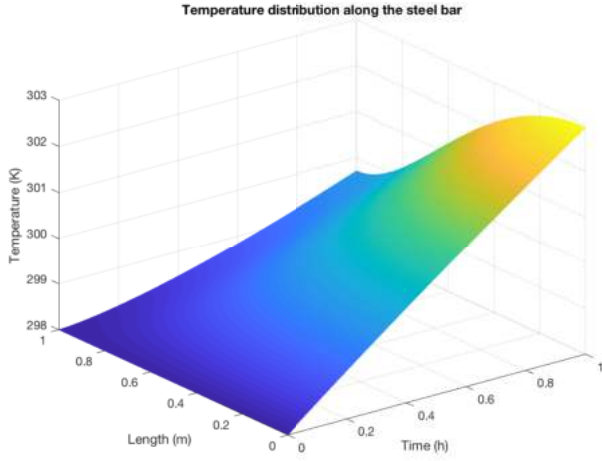


Fig. 2. Simulation results via FEM of the PDE in (19).

Now, in the following, we design the observer via the LSD method. Considering a finite, one-dimensional spatial domain and the boundary conditions, the basis $\phi_i(x)$ are

$$\phi_i(x) = \begin{cases} 1, & i = 1 \\ \sqrt{2} \cos([(i-1)\pi x]), & i \geq 2. \end{cases}$$

In turn the respective eigenvalues are

$$\lambda_i = -[(i-1)\pi]^2,$$

and the weights of the source term are given by

$$w_i = \frac{q_0}{\rho c} \begin{cases} \frac{2}{3}, & i = 1 \\ (-1)^i \frac{2^{3/2}}{[(i-1)\pi]^2}, & i \geq 2. \end{cases}$$

Now, in the following, we design a discrete-time observer based on Equation (13). Please recall that $\hat{\mathbf{z}}[t, \mathbf{x}] = \mathbf{\Phi}^\top[\mathbf{x}] \hat{\mathbf{w}}_{\mathbf{z}}(t)$, where $\mathbf{\Phi}^\top[\mathbf{x}]$ is as in (9). In addition, the spatial discretisation we consider is $\mathbf{x} = \left(L \frac{i}{51} \right)_{i=1}^{51}$ and avail of the first 4 elements in the basis $\phi_i(x)$ of the spatial domain. Hence $\vartheta = 4$.

Furthermore, we assume that the measurements we have available are at the extreme of the bar; thus, $\mathbf{x}_m = (0 \ 1)^\top$. Accordingly, the matrix \mathbf{C} is a 2×51 matrix, whose elements are all zeroes, except the 1,1 and the 2,51.

In turn, our sampling period is $\tau = 1$. This value along with the previously defined eigenvalues λ_i lead to

$$\mathbf{A}_d = \text{diag} \left(\left\{ 1 - \frac{k}{\rho c} [(i-1)\pi]^2 \right\}_{i=1}^4 \right).$$

The LMIs (B.3a) and (B.4) were solved using the solver *SEDUMI* over the *Yalmip* toolbox (Löfberg, 2004). The observer gain computed was

$$\mathbf{L}_d = \begin{pmatrix} 0.2149 & 0.2149 \\ 0.1958 & -0.1958 \\ 0.2004 & 0.2004 \\ 0.1525 & -0.1525 \end{pmatrix}.$$

In this light, the estimated values of the temperature at the locations \mathbf{x} , given the measurements at the locations \mathbf{x}_m are depicted in Figure 3. In turn, the difference between the FEM solution and the estimation arising from our observer may be found in Figure 4. Please notice that the error of the estimate and the actual temperature is rather small in comparison to the signal's value.

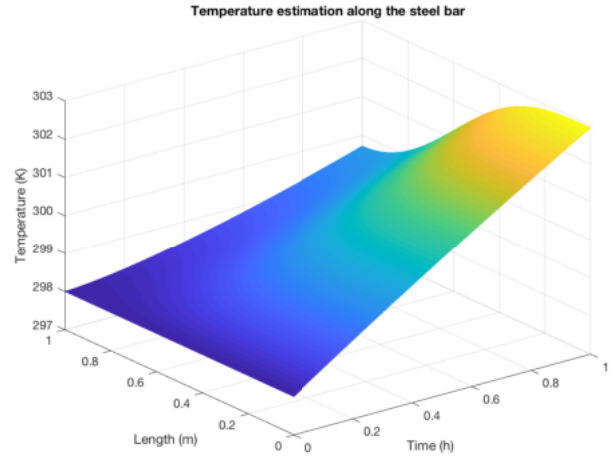


Fig. 3. Estimated temperatures using the discrete observer in Equation (13).

6. CONCLUSIONS

We considered a continuous-time, continuous-space, uni-dimensional heat equation, and assumed that we avail of measurements at particular locations within the spatial domain. Our task was to estimate the field value at unmeasured locations. To this end, we approximated the solution of the PDE by means of a discrete space and discrete-time model. An observer was then proposed as a copy of this reduced model plus a linear correction term. We provide the rigorous convergence proof to the actual states, provided the observability of the pair $(\mathbf{A}_d, \mathbf{C}_e)$.

Results showed that the reduced model-based observer is able to correctly estimate the temperature profile along

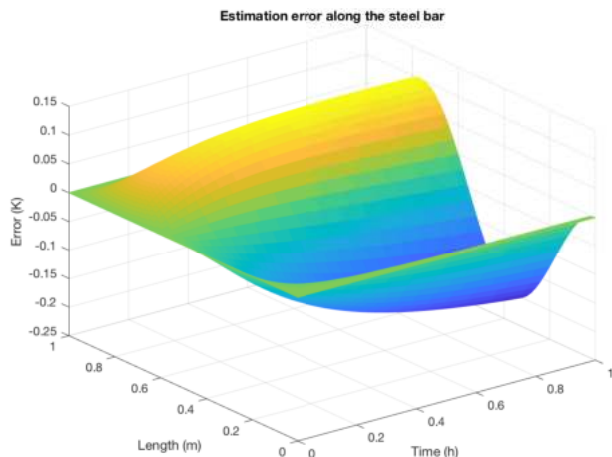


Fig. 4. Estimation error.

the bar with a maximum error of 0.1 K by using only measurements at the extreme locations of the steel bar. It must be highlighted that the error was propagated along the space domain according to the truncation of the basis used. That is to say, the smaller the number of basis element used, the larger the estimation error, given that one neglects the input of the disregarded basis elements. This suggests that the number of basis functions must be selected carefully in order to reach a small estimation error.

On the other hand, since the observer proposed is a low order difference equation system, it can be embedded in a digital system (microcontroller, FPGA, etc.). The estimation strategy proposed is therefore a promising method for real applications in industry.

ACKNOWLEDGMENTS

This work was supported by the UG program PFCE 2019. S. Cano-Andrade thanks to Rosalba P. Hernandez-Luquin from the Mechanical Engineering Department of the Universidad de Guanajuato for fruitful discussions during the development of this manuscript, and to CONACyT for its financial support under the SNI program.

REFERENCES

Bianchi, M.F., Gameros, A.A., Axinte, D.A., Lowth, S., Cendrowicz, A.M., and Welch, S.T. (2019). On the effect of mould temperature on the orientation and packing of particles in ceramic injection moulding. *Journal of the European Ceramic Society*, 39(10), 3194 – 3207.

Chandrupatla, T.R., Belegundu, A.D., Ramesh, T., and Ray, C. (2002). *Introduction to finite elements in engineering*, volume 10. Prentice Hall Upper Saddle River, NJ.

Christofides, P.D. (2012). *Nonlinear and robust control of PDE systems: Methods and applications to transport-reaction processes*. Springer Science & Business Media.

Courant, R. and Hilbert, D. (1937). *Methods of Mathematical Physics*.

Demirel, B. (2017). Optimisation of mould surface temperature and bottle residence time in mould for the carbonated soft drink pet containers. *Polymer Testing*, 60, 220 – 228.

Fan, Z. and Gao, R.X. (2006). A dual sensing approach to simultaneous temperature and pressure measurement from injection mold cavity. In *ASME 2006 International Mechanical Engineering Congress and Exposition*, 841–847. American Society of Mechanical Engineers.

García, M.R. (2008). *Identification and real time optimization in the food processing and biotechnology industries*. Ph.D. thesis, Universidade de Vigo.

García, M.R., Vilas, C., Banga, J.R., and Alonso, A.A. (2007). Optimal field reconstruction of distributed process systems from partial measurements. *Industrial & Engineering Chemistry Research*, 46(2), 530–539.

Goodship, V. (2004). *Troubleshooting Injection Moulding*. Rapra Technology Limited.

Grebenkov, D. and Nguyen, B. (2013). Geometrical structure of laplacian eigenfunctions. *SIAM Review*, 55(4), 601–667.

Hidayat, Z., Babuska, R., De Schutter, B., and Nunez, A. (2011). Observers for linear distributed-parameter systems: A survey. In *2011 IEEE International Symposium on Robotic and Sensors Environments (ROSE)*, 166–171. IEEE.

Hwang, K. (2012). *10 Common defects in metal injection molding (MIM)*. Woodhead Publishing.

Jiang, J., Wang, S., Sun, B., Ma, S., Zhang, J., Li, Q., and Hu, G.H. (2015). Effect of mold temperature on the structures and mechanical properties of micro-injection molded polypropylene. *Materials and Design*, 88, 245 – 251.

Llu, Y.A. and Lapldus, L. (1976). Observer theory for distributed-parameter systems. *International Journal of Systems Science*, 7(7), 731–742. doi: 10.1080/00207727608941960.

Löfberg, J. (2004). Yalmip : A toolbox for modeling and optimization in MATLAB. In *Proc CACSD Conference*. Taipei, Taiwan. URL <http://users.isy.liu.se/johanl/yalmip>.

López-Caamal, F. and Moreno, J.A. (2015). Observación de sistemas de reacción difusión con tasas de reacción afines. In *Congreso Nacional de Control Automático*. Cuernavaca, Mexico.

Mamoun, A.A. and Tapan, K. (2015). Proportional integral control approach for controlling the temperatures of multi-steel cylinders barrel in an injection molding machine. *ASME International Mechanical Engineering Congress and Exposition*, 4A Dynamics, Vibration, and Control, 1–5.

Renterghem, J.V., Dhondt, H., Verstraete, G., Bruyne, M.D., Vervaet, C., and Beer, T.D. (2018). The impact of the injection mold temperature upon polymer crystallization and resulting drug release from immediate and sustained release tablets. *International Journal of Pharmaceutics*, 541(1), 108 – 116.

- Ronkay, F., Molnar, B., and Dogossy, G. (2017). The effect of mold temperature on chemical foaming of injection molded recycled polyethylene-terephthalate. *Thermochimica Acta*, 651, 65 – 72.
- Scherer, C. and Weiland, S. (2004). *Linear Matrix Inequalities in Control*. Delft University of Technology.
- Torres, I., Queinnec, I., Vilas, C., and Vande Wouwer, A. (2010). Observer-based output feedback linear control applied to a denitrification reactor. In *American Control Conference (ACC), 2010*, 5880–5885. IEEE.
- Vilas Fernández, C. (2008). *Modelling, simulation and robust control of distributed processes: application to chemical and biological systems*. Ph.D. thesis, Universidade de Vigo.
- Wouwer, V. and Zeitz, M. (2009). State estimation in distributed parameter systems. *Control Systems, Robotics and Automation—Volume XIV: Nonlinear, Distributed, and Time Delay Systems-III*, 92.
- Zheng, Y., Gu, F., Ren, Y., Hall, P., and Miles, N.J. (2017). Improving mechanical properties of recycled polypropylene-based composites using taguchi and anova techniques. *Procedia CIRP*, 61, 287 – 292.
- Zuazua, E. (2007). Controllability and observability of partial differential equations: some results and open problems. In *Handbook of differential equations: evolutionary equations*, volume 3, 527–621. Elsevier.

Appendix A. PROOF OF PROPOSITION 1

Here we provide the convergence proof of observer (12). To this end, let us consider Equation (8) and express it in the approximation (4) to obtain:

$$\frac{d}{dt} \left(\mathbf{w}_z^\top(t) \phi(x) \right) = \alpha \nabla^2 \left(\mathbf{w}_z^\top(t) \phi(x) \right) + f(t, x).$$

By availing of the properties of the elements of $\phi(x)$ and applying the inner product with the vector $\phi(x)$, one obtains

$$\frac{d}{dt} \mathbf{w}_z(t) = \mathbf{A} \mathbf{w}_z(t) + \mathbf{w}_f(t), \quad (\text{A.1})$$

where \mathbf{A} is as in (10) and the elements of $\mathbf{w}_f(t)$ are as in (3). Likewise,

$$\mathbf{y}(t, x) \approx \phi(x)^\top \mathbf{w}_z(t) \quad (\text{A.2})$$

Thus by defining $\mathbf{e}(t) := \hat{\mathbf{w}}_z(t) - \mathbf{w}_z(t)$ and accounting for System (12), the observation error dynamics become

$$\frac{d}{dt} \mathbf{e}(t) = (\mathbf{A} - \mathbf{L} \mathbf{C}_e) \mathbf{e}(t),$$

which might be rendered stable via a suitable \mathbf{L} , given the observability of the pair $(\mathbf{A}, \mathbf{C}_e)$.

Appendix B. PROOF OF PROPOSITION 2

As described in Appendix A, the dynamics of the plant may be approximated via

$$\frac{d}{dt} \mathbf{w}_z(t) = \mathbf{A} \mathbf{w}_z(t) + \mathbf{w}_f(t), \quad (\text{A.1})$$

which we discretize by Euler approximation, leading to the following difference equation

$$\hat{\mathbf{w}}_z[k+1] = \mathbf{A}_d \hat{\mathbf{w}}_z[k] + \tau \mathbf{w}_f[k], \quad (\text{B.1})$$

where \mathbf{A}_d is as in (14a). By considering (13) and defining the observation error as

$$\mathbf{e}[k] := \hat{\mathbf{w}}_z[k] - \mathbf{w}_z[k],$$

one may see that the discrete-time error dynamics are given by

$$\begin{aligned} \mathbf{e}[k+1] &= \mathbf{A}_d \mathbf{e}[k] - \mathbf{L}_d (\hat{\mathbf{y}}[k, \mathbf{x}_m] - \mathbf{y}[k, \mathbf{x}_m]), \\ &= \mathbf{A}_d \mathbf{e}[k] - \mathbf{L}_d \mathbf{C}_e (\hat{\mathbf{w}}_z[k] - \mathbf{w}_z[k]), \\ &= (\mathbf{A}_d - \mathbf{L}_d \mathbf{C}_e) \mathbf{e}[k]. \end{aligned}$$

The stability of the observation error origin's may be attained by choosing an appropriate \mathbf{L}_d , provided that the pair $(\mathbf{A}_d, \mathbf{C}_e)$ is observable.

In order to compute the observer gain \mathbf{L}_d , let us now consider the following candidate Lyapunov function

$$V(\mathbf{e}) = \mathbf{e}^\top \mathbf{P} \mathbf{e}, \quad (\text{B.2})$$

with $\mathbf{P} = \mathbf{P}^\top$ (Scherer and Weiland, 2004). The derivative of $V(\mathbf{e})$ with respect to time is given by

$$\begin{aligned} \dot{V}(\mathbf{e}) &= \lim_{\tau \rightarrow 0} \frac{\Delta V}{\tau} = \lim_{\tau \rightarrow 0} \frac{V(\mathbf{e}[k+1]) - V(\mathbf{e}[k])}{\tau} \\ &= \lim_{\tau \rightarrow 0} \frac{\mathbf{e}^\top[k] \left[(\mathbf{A}_d - \mathbf{L}_d \mathbf{C}_e)^\top \mathbf{P} (\mathbf{A}_d - \mathbf{L}_d \mathbf{C}_e) - \mathbf{P} \right] \mathbf{e}[k]}{\tau}. \end{aligned}$$

Clearly, (B.2) is a Lyapunov function if and only if

$$\mathbf{P} > 0 \quad (\text{B.3a})$$

$$(\mathbf{A}_d - \mathbf{L}_d \mathbf{C}_e)^\top \mathbf{P} (\mathbf{A}_d - \mathbf{L}_d \mathbf{C}_e) - \mathbf{P} < 0, \quad (\text{B.3b})$$

This way the asymptotic stability of the estimation error is assured and therefore, the estimated weight $\hat{\mathbf{w}}_z$ asymptotically will converge to the true weight \mathbf{w}_z . By considering the change of variable $\mathbf{Q} = \mathbf{P} \mathbf{L}_d$ and by applying the Schur complement to the matrix inequality (B.3b) the following linear matrix inequality (LMI) is obtained

$$\begin{bmatrix} -\mathbf{P} & \mathbf{A}_d^\top \mathbf{P} - \mathbf{C}_e^\top \mathbf{Q}^\top \\ \mathbf{P} \mathbf{A}_d - \mathbf{Q} \mathbf{C}_e & -\mathbf{P} \end{bmatrix} < 0. \quad (\text{B.4})$$

By solving LMIs (B.3a) and (B.4) for \mathbf{P} and \mathbf{Q} , the observer gain is computed as $\mathbf{L}_d = \mathbf{P}^{-1} \mathbf{Q}$.